Available online at www.sciencedirect.com

ScienceDirect

journal homepage: www.intl.elsevierhealth.com/journals/dema

Antibacterial response of oral microcosm biofilm to nano-zinc oxide in adhesive resin

Isadora Martini Garcia[a,b], *AbdulRahman A. Balhaddad*[c,d], *Maria S. Ibrahim*[e], *Michael D. Weir*[b,c], *Hockin H.K. Xu*[b,c,*], *Fabrício Mezzomo Collares*[a,**], *Mary Anne S. Melo*[c,f,*]

[a] *Dental Materials Laboratory, School of Dentistry, Federal University of Rio Grande do Sul, Porto Alegre, RS, Brazil*
[b] *Division of Biomaterials and Tissue Engineering, Department of Advanced Oral Sciences and Therapeutics, University of Maryland School of Dentistry, Baltimore, MD 21201, USA*
[c] *Ph.D. Program in Dental Biomedical Sciences, University of Maryland School of Dentistry, Baltimore, MD 21201, USA*
[d] *Department of Restorative Dentistry, Umm Al-Qura University, College of Dentistry, Makkah, Saudi Arabia*
[e] *Department of Preventive Dental Sciences, College of Dentistry, Imam Abdulrahman Bin Faisal University, Dammam, Saudi Arabia*
[f] *Operative Dentistry Division, General Dentistry Department University of Maryland School of Dentistry, Baltimore, MD 21201, USA*

ARTICLE INFO

Article history:
Received 16 January 2020
Accepted 26 November 2020

Keywords:
Dentin-bonding agents
Antibacterial agents
Biofilms
Dental caries
Composite resins
Polymers

ABSTRACT

Objective. Various nanoparticles are currently under investigation to impart biointeractivity for dental materials. This study aimed to: (1) formulate an experimental dental adhesive containing ZnO nanoparticles; (2) evaluate its chemical and mechanical properties; and (3) assess the antibacterial response against oral microcosm biofilm.

Methods. Nanosized ZnO was chemically and morphologically evaluated. ZnO was incorporated at 0 (G_{CTRL}), 2.5 ($G_{2.5\%}$), 5 ($G_{5\%}$) and 7.5 ($G_{5\%}$) wt.% in an experimental dental adhesive. The adhesives were evaluated for the degree of conversion (DC), flexural strength (FS), and elastic modulus (E). The antibacterial activity was evaluated using a 48 h-microcosm biofilm model after the formation of acquired pellicle on samples' surfaces. Colony-forming units (CFU), metabolic activity, and live/dead staining were assessed.

Results. Nanosized ZnO presented characteristic peaks of Zn-O bonds, and the particles were arranged in agglomerates. The DC ranged from 62.21 (±1.05) % for G_{Ctrl} to 46.15 (±1.23) % for $G_{7.5\%}$ ($p < 0.05$). $G_{7.5\%}$ showed lower FS compared to all groups ($p < 0.05$). Despite achieving higher E ($p < 0.05$), $G_{2.5\%}$ did not show differences for G_{Ctrl} regarding the FS ($p > 0.05$). $G_{7.5\%}$ had lower CFU/mL compared to G_{Ctrl} for mutans streptococci ($p < 0.05$) and total microorganisms ($p < 0.05$), besides presenting lower metabolic activity ($p < 0.05$) and higher dead bacteria via biofilm staining.

* *Corresponding authors at*: 650 West Baltimore St., Baltimore, MD 21201, USA.
** *Corresponding author at*: Rua Ramiro Barcelos, 2492, 90035-003 Porto Alegre, RS, Brazil.
E-mail addresses: isadora.garcia@ufrgs.br (I.M. Garcia), abalhaddad@umaryland.edu (A.A. Balhaddad), msibrahim@iau.edu.sa (M.S. Ibrahim), michael.weir@umaryland.edu (M.D. Weir), hxu@umaryland.edu (H.H.K. Xu), fabricio.collares@ufrgs.br (F.M. Collares), mmelo@umaryland.edu (M.A.S. Melo).
https://doi.org/10.1016/j.dental.2020.11.022
0109-5641/© 2020 The Academy of Dental Materials. Published by Elsevier Inc. All rights reserved.

Significance. The dental adhesives' physicochemical properties were similar to commercial adhesives and in compliance with ISO recommendations. $G_{7.5\%}$ restricted the growth of oral microcosm biofilm without impairing the physicochemical performance.

© 2020 The Academy of Dental Materials. Published by Elsevier Inc. All rights reserved.

1. Introduction

Increasing demand for improved long-term performance of dental adhesives has led to intense investigations on strategies for them to express biointeractivity [63]. In this way, dental adhesives may have the potential to improve the longevity of the bonding interface by reducing dental plaque or promoting bioactivity [3–7]. Besides antibacterial activity and stimulation of dentin remineralization, dental adhesives aimed to be modified to present higher hydrolytic stability and to inhibit collagen degradation by endogenous proteases [6].

Many types of nanoparticles have emerged as a new class of inorganic agents due to their pronounced effect in reducing bacterial proliferation [7]. As bioactive agents, nanoparticles can facilitate mineral growth with a direct result in bonding interface degradation [8]. Zinc oxide (ZnO) nanoparticles have attracted much consideration due to their multifaceted and promising applications [9]. In dentistry, this oxide presented in microsized particles has well-recognized use in sealers and cements (zinc oxide-eugenol and zinc phosphate cements) [10]. Some researchers have oriented studies toward bioactivity promoted by zinc oxides [11,12]. Nevertheless, ZnO nanoparticles present not only bioactivity via the formation of calcium phosphates on its surface [11] and excellent biocompatibility [13], but also can negatively affect metalloproteinases [6] and oral bacteria [14–18].

The antimicrobial behavior of nanoparticles is mainly due to their smaller size and the high surface area to volume ratio, i.e., the the nanoparticle's large surface area enhances their interaction with the bacteria to carry out broad-spectrum antibacterial efficacy [19]. ZnO nanoparticles have shown bactericidal effects on Gram-positive and Gram-negative oral bacteria, as well as against fungal spores [14,20,21]. Specifically, studies have demonstrated the superior antimicrobial activity of ZnO nanoparticles against *Streptococcus mutans* in comparison to ZnO in the particle size range of microns [22]. Moreover, the literature has shown that ZnO nanoparticles have toxicity toward bacteria andhave minimal effect on human cells [23]. These outcomes are exciting and can help investigators determine whether a candidate nanoparticle has scientific merit to justify further applicability.

Currently, a glance at the current literature reveals that antibacterial investigations on ZnO in adhesives have been performed by agar diffusion tests [20,24], direct contact tests with 8 or 24 h to evaluate the biofilm formation [14,18,21,25,26] or the planktonic cells' viability [27]. Even though many studies previously evaluated ZnO's harmful activity against oral microorganisms, the designs are usually simple compared to the intra-oral environment Bacterial biofilms inside the mouth present a more complex physical structure [28] and occur with high resistance against antibacterial agents than their free-living counterparts [29]. Besides the concern about the complexity of the biofilm model used, other conditions related to these interactions are not reproduced in vitro, such as the formation of salivary acquired pellicle on the surface of restorative materials [30]. In vitro assays, using more complex biofilm models could help understand materials' properties and help in the translation of knowledge from bench to clinical setting [31].

A growing awareness of the limitations of using single oral bacterial species, immature biofilms, and its inability to make reliable predictions led us to investigate nano-ZnO properties using a more complex biofilm model [31]. In the process of tuning nano-ZnO in dental resins, one potential strategy to overcome the challenge faced by treating biofilms is to increase the concentration of the chosen agent. Conflicting with this approach, high concentrations of inorganic fillers may reduce the adhesive's curing potential and jeopardize the mechanical properties. This study aimed to: (1) formulate an experimental dental adhesive containing ZnO nanoparticles; (2) evaluate its chemical and mechanical properties; and (3) assess the antibacterial response against human saliva-based oral microcosm biofilm.

2. Materials and methods

Nanoparticles of ZnO powder were initially appraised for chemical and morphological characterization. Further independent studies for their chemical, physical, and antibacterial properties were conducted using experimental dental adhesives containing ZnO nanoparticles. Fig. 1 depicts a schematic diagram of the experimental design and the steps of assessments pipeline employed in this study.

2.1. *Chemical and morphological characterization of ZnO*

A commercially available nanopowder of ZnO was used in this study (Aldrich Chemical Company, St. Louis, Missouri, USA). In order to chemically characterize the powder of ZnO, Fourier Transform Infrared Spectroscopy (FTIR) and micro-Raman spectroscopy were used. For FITR analysis (Vertex 70, Bruker Optics, Ettlingen, Germany), the powder of ZnO was directly placed on the attenuated total reflectance device (ATR). Opus 6.5 software (Bruker Optics, Ettlingen, Germany) was used for processing the spectra in the range from 400 to 3000 cm^{-1} using 16 scans and 4 cm^{-1} of resolution. For micro-Raman spectroscopy (SENTERRA, Bruker OptikGmbH, Ettlingen, Baden-Württemberg, Germany), a 100 mW diode laser with wavelength at 785 nm and a spectral resolution of ~3.5 cm^{-1} were used. The spectra were obtained in the range from 70 to 1500 cm^{-1} with three co-additions per 2 s.

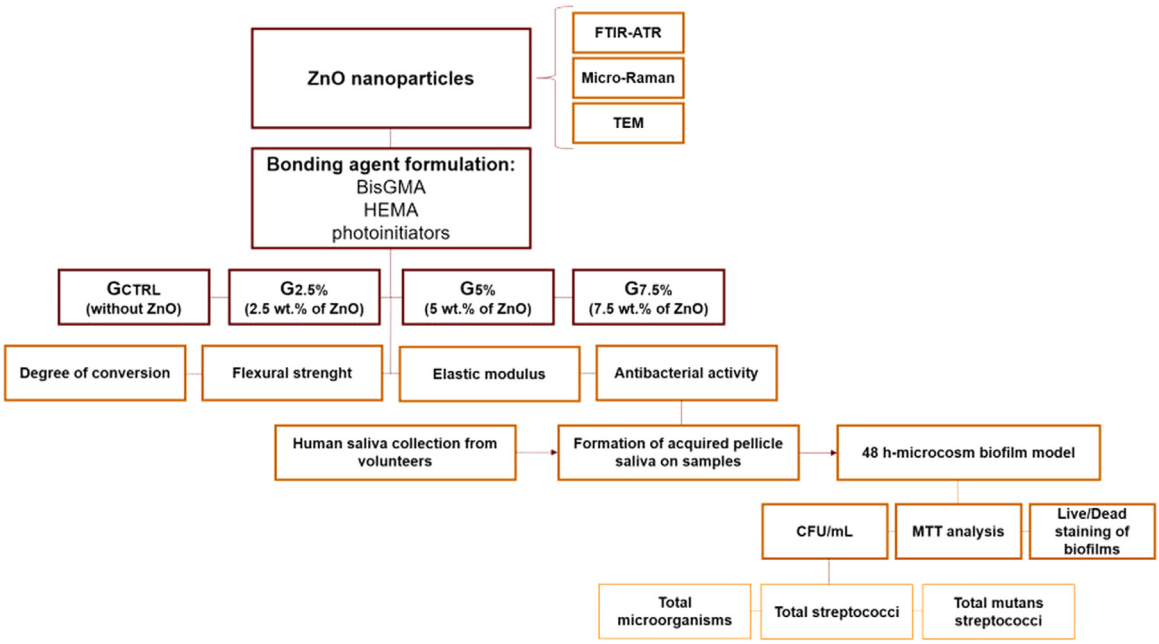

Fig. 1 – Flowchart of the experimental design purposed in this study. There was a phase for ZnO characterization, followed by dental adhesives formulation. Then, the resins were chemically and physically evaluated. Finally, the antibacterial activity was analyzed using microcosms biofilm model from saliva-derived inoculum, formation of acquired pellicle from saliva and maturation of biofilm for 48 h. The ability to inhibit the biofilm formation on dental adhesives surfaces was evaluated via colony formaing units couting (CFU/mL), metabolic activity via MTT analysis and live/dead staining of biofilms.

Transmission electron microscopy (TEM) was used after mixing ZnO powder with water to evaluate the nano-ZnO morphological features. The nanoparticle solution was dropped (15 μL) onto a 300-mesh carbon-coated copper grid (Ted Pella, Redding, CA, USA). The TEM (FEI Tecnai T20, Hillsboro, OR) equipped with the Software Imaging System CCD camera (Gatan UltraScan 1000) was performed at 80 kV with a magnification of 30,000× and 110,000×, and 200 particles were counted by measuring each one in two axes (400 counts).

2.2. *Experimental formulations of dental adhesives*

The formulations of experimental dental adhesives contain 66.66 wt.% of bisphenol A glycerolate dimethacrylate (BisGMA) manually mixed with 33.33 wt.% of 2-hydroxyethyl methacrylate (HEMA). Camphorquinone and ethyl 4-dimethylaminobenzoate at 1 mol% were added as a photoinitiator system. Butylated hydroxytoluene was added at 0.01 wt.% as a polymerization inhibitor [33,34]. ZnO was incorporated at 2.5, 5, and 7.5 wt.% in the experimental formulation to obtain three test groups: $G_{2.5\%}$, $G_{5\%}$, and $G_{7.5\%}$. One group remained without the ZnO addition to being used as control (G_{Ctrl}). The formulations were mixed using a mechanical mixer (DAC 150 Speed mixer, Flacktek, Landrum, SC, USA) at 2800 rpm for 1 min. All reagents used for the formulations were purchased from Aldrich Chemical Company (St. Louis, Missouri, USA) and used without further purification.

2.3. *Degree of conversion*

The degree of conversion (DC) of each dental adhesive ($n = 5$) was measured via FTIR-ATR (Nicolet 6700, Thermo Fisher Scientific, Waltham, Massachusetts, USA). The dental adhesives were dispensed on the ATR crystal using a mold of polyvinylsiloxane to standardize samples' thickness in 1 mm. Each sample was covered with a polyester strip and photoactivated during 20 s using a light-curing unit with 1000 mW/cm^2 (VALO Cordless, Ultradent Products, South Jordan, Utah, USA) and the tip as close as possible to the top of the sample. Each sample was analyzed before and after the photoactivation. The data were evaluated using OMNIC Series Software (Thermo Fisher Scientific), from 400 to 4000 cm^{-1}, with 32 scans and 4 cm^{-1} of resolution. We considered the intensity of the aliphatic carbon-carbon double bond (1638 cm^{-1}) and the aromatic carbon-carbon double bond (1608 cm^{-1}) [35] from the dental adhesives to calculate the DC. Values before and after the photoactivation following the equation:

$$\text{DC} \quad (\%) = 100 \times \left(\frac{\text{peak height of cured aliphatic C = C/peak height of cured aromatic C = C}}{\text{peak height of uncured aliphatic C = C/peak height of uncured aromatic C = C}} \right)$$

2.4. Flexural strength and flexural modulus

Samples of each group ($n = 10$) were prepared ($2 \times 2 \times 25$ mm), and the flexural strength and the flexural modulus were examined [36]. Polyester strips were applied at the top and the bottom of each sample, and then, the samples were photoactivated (Valo grand, Ultradent Products Inc, South Jordan, UT, USA; standard mode; 1029 mW/cm^2) for 20 s on each side. The adhesive samples were stored at 37 °C for 24 h with distilled water. Three-point flexure with a 10 mm span and crosshead-speed of 1 mm/min (MTS 5500R, Cary, NC, USA) was used to examine the flexural strength and the flexural modulus of each sample. The following equation (2) was used to calculate the flexural strength (F):

$$F \quad (\text{MPa}) = \left(\frac{3LS}{2WH^2} \right) \tag{2}$$

In Eq. (2), L is the maximum load; S is the span; W is the width of the specimen, and H is the height.

For the elastic modulus (E), the values were obtained by the following equation (3):

$$E \quad (\text{MPa}) = \left(\frac{LS^2 3}{4WH^2 3d} \right) \tag{3}$$

In Eq. (3), L is the maximum load; S is the span; W is the width of the specimen, H is the height of the specimen, and d is the defluxion corresponding to the load L.

2.5. Preparation of samples for microbiological assays

Disk-shape samples were prepared with 9 mm of diameter and 1 mm of thickness. The samples were photoactivated for 20 s on each side, and the excesses around were gently removed with sandpaper (2000-grit) under distilled water irrigation. The samples were kept in distilled water at 37 °C for 24 h, sterilized using ethylene oxide gas (AnproleneAN 74i, Andersen, Haw River, NC, USA), and de-gassed for seven days.

2.6. Saliva collection from healthy volunteers

The whole saliva from ten healthy volunteers was collected on ice to prepare the inoculum used for all the performed microbiological assays. The use of human saliva was approved by the University of Maryland Baltimore Institutional Review Board (HP-00050407) and performed according to the previous study [37]. Saliva was used to form an acquired pellicle on material surfaces and as a bacterial inoculum for the microcosm biofilm model [37]. The volunteers had natural dentition, no active caries, and they did not use antibiotics within the past three months. The ten volunteers were instructed to avoid tooth brushing for 24 h and not eat or drink for two hours before the collection. Chewing parafilm were distributed and the volunteers were asked to chew for 1 min and dispense the saliva. Then, the volunteers continued chewing and collecting the saliva in a sterilized falcon tube for 5 min, which was kept inside a recipient with ice. For bacterial inoculum, saliva from all the volunteers was mixed and then centrifuged for 20 min at 4000 rpm. The supernatant was removed to be mixed with glycerol (70 % saliva/30 % glycerol) following previous work [38]. All samples were stored a −80 °C for subsequent use.

The saliva inoculum was mixed at 1:50 proportion with McBain medium containing mucin (Type II, porcine, gastric) at 2.5 g/L; bacteriological peptone at 2.0 g/L; tryptone at 2.0 g/L; yeast extract at 1.0 g/L; NaCl at 0.35 g/L; KCl at 0.2 g/L; $CaCl_2$ at 0.2 g/L; cysteine hydrochloride at 0.1 g/L; hemin at 0.001 g/L; vitamin K_1 at 0.0002 g/L in the final adjustment of pH at 7 [39]. Sterilized sucrose at 0.2 wt.% was also added to McBain broth.

2.7. Acquired salivary pellicle formation on samples

To simulate the saliva absorbed onto dental material surfaces to provide anchor points for bacteria. For acquired pellicle formation, saliva was diluted 1:1 with adsorption buffer and supplemented with the protease inhibitor phenylmethylsulfonyl fluoride (1.0 mmol/L final concentration) and then centrifuged at 4000 rpm for 10 min at 4 °C. The diluted saliva solutions were filtered by 0.22 μm-filter (Millipore Corporation, Massachusetts, USA). The pH was adjusted to 6.5. The clear and filter-sterilized saliva solution were pooled and used for pellicle formation. Each adhesive sample was independently immersed in clarified saliva and incubated over 2 h at room temperature (24 ± 1 °C) before the microcosm biofilm model.

2.8. Microcosm biofilm model

After the formation of the acquired salivary pellicle, the samples ($n = 6$) were gently placed on sterile 24-well plates with 1.5 mL of a solution composed of McBain and saliva with glycerol (1/50 proportion). The 24-well plates were kept at 37 °C with 5% CO_2. After 8 and 24 h, the samples were placed on new 24-well plates with 1.5 mL of McBain without saliva. The samples were kept for more than 24 h in contact with McBain, totalizing 48 h of biofilm formation at 37 °C in a microaerophilic environment containing 5% of CO_2.

2.9. Colony-forming unit (CFU) counts of biofilms

After 48 h of biofilm formation after treatment, suspensions were serially diluted in CPW salt solution (yeast extract at 5 g/L; peptone at 1 g/L; NaCl at 9.5 g/L; cysteine hydrochloride at 0.5 g/L). In order to assess bacterial viability, 0.1 mL aliquots of each dilution were plated in triplicate To determine microorganisms viability, samples were plated in triplicate on the following culture media: mitis salivarius agar, containing 15 % sucrose, to determine total streptococci; MSA agar plus 0.2 units of bacitracin/ml) to determine mutans streptococci, and tryptic soy blood agar (TSA) supplemented with 5 % of blood to determine total microorganisms. The plates were incubated for 48 h at 37 °C in a partial atmosphere of 5 % CO_2. Represen-

tative colonies of mutans streptococci, total streptococci, and total microorganisms were counted using a colony counter, and the results were expressed as colony-forming units per milliliter (CFU/mL).

2.10. MTT assay of metabolic activity of biofilms

A colorimetric assay was conducted to analyze the enzymatic reduction of 3-[4,5-dimethylthiazol-2-yl]-2,5-diphenyltetrazolium bromide (MTT) to evaluate the metabolic activity. After 48 h of biofilm maturation, six samples per group were transferred to a 24-well plate containing 1 mL of a earlier prepared solution containing 0.5 mg/mL of MTT in phosphate-buffered saline (PBS, NaCl at 8 g/L; KCl at 0.2 g/L; Na_2HPO_4 at 1.44 g/L; KH_2PO_4 at 0.24 g/L). The plate was kept for 1 hour at 37 °C and 5% of CO_2. The samples were transferred to a new 24-well plate with 1 mL of dimethyl sulfoxide (DMSO) to solubilize the crystals. The plate was kept under room temperature, for 20 min, in a dark environment. Then, 200 μL from each well was transferred to a 96-well plate, and the absorbance was measured at 540 nm wavelength (SpectraMax M5, Molecular Devices, Sunnyvale, CA, USA).

2.11. Microscopy evaluation of biofilms via live/dead assay

For the live/dead assay, one sample per group was qualitatively evaluated using an inverted epifluorescence microscope (Eclipse TE2000-S, Nikon, Melville, NY, USA). First, the samples were removed from the plate after 48 h of biofilm maturation and gently washed by immersing them in PBS. Then, the samples were positioned on a filter paper to let remove the excess of PBS and stained with BacLight live/dead kit (Molecular Probes, Eugene, OR, USA). A mixture of SYTO 9 and propidium iodide (2.5 μM of each one) was used to stain the discs for 15 min. SYTO9 was used to stain live bacteria using 483 nm of wavelength. The fluorescence of live bacteria is presented at 503 nm (green). Propidium iodide was used to stain bacteria with defects in their membranes using 535 nm of wavelength and presenting fluorescence in 617 nm (red).

2.12. Statistical analysis

The distribution of data was analyzed by the Shapiro–Wilk test. One-way ANOVA and Tukey post hoc tests were used for all quantitative tests at a level of 0.05 of significance. The regression line that best fits the scatter plot of DC versus ZnO concentration was plotted. The level of correlation between the DC and ZnO concentration was analyzed using Spearman's correlation test. The statistical analyses were performed via the software SigmaPlot® with version 12.0 (Systat Software, Inc., San Jose, CA, USA).

3. Results

Fig. 2 presents the results of the chemical and morphological characterization of ZnO. The spectra analyses (Fig. 2A and B) show the peaks related to Zn—O bond at 410 cm^{-1} for FTIR [40] and at 442 cm^{-1} [41], 333 cm^{-1} [42] and 97 cm^{-1} [43] for micro-Raman. TEM analysis (Fig. 2C–E) indicated that the nanoparticles presented a very irregular pattern of shape. Spherical, hexagonal, and long shape particles could be observed. ZnO powder was mainly arranged in agglomerates of nanoparticles. The distribution of particle size is shown in Fig. 2F, indicating a non-normal distribution, with a mean particle size of 51.08 (±32.13) nm and a median of 42.34. The 25th percentile was 29.58 nm. and the 75th percentile was 63.94 nm, with a minimum value of 15.31 nm and a maximum value of 270.03 nm.

The results of DC are plotted in Fig. 3. In Fig. 3A, the chemical structure of BisGMA and HEMA. In Fig. 3B, changes on the peaks (C=C bond of aliphatic chain at 1640 cm^{-1}) differences between monomer and polymer were noted. In Fig. 3C, the DC results ranged from 62.21 (±1.05) % for G_{CTRL} to 45.15 (±1.23) % for $G_{7.5\%}$, with statistical differences among groups ($p < 0.05$). A strong and significant ($p < 0.001$) negative correlation was observed between ZnO concentration and DC (Spearman correlation coefficient = −0.946), as observed in Fig. 3D.

Fig. 4A shows the results of flexural strength. The values ranged from 107.45 (±16.41) MPa for G_{CTRL} to 84.57 (±21.82) MPa for $G_{7.5\%}$ ($p < 0.05$). Up to 5 wt.% of ZnO addition, there was no difference compared to G_{CTRL} ($p > 0.05$). The group with 7.5 wt.% of ZnO showed a lower value compared to G_{CTRL} ($p < 0.05$) without difference for $G_{5\%}$ (100.41 ± 14.50 MPa). Fig. 4B shows the values of elastic modulus, which ranged from 4698.07 (±703.17) MPa for $G_{2.5\%}$ to 3546.58 (±652.09) MPa for $G_{7.5\%}$ ($p < 0.05$). $G_{2.5\%}$ showed higher value compared to G_{CTRL} (3613.11 ± 445.52 MPa) and $G_{7.5\%}$ ($p < 0.05$), without statistical difference between $G_{2.5\%}$ and $G_{5\%}$ ($p > 0.05$).

Fig. 5 presents the results of all microbiological assays performed to evaluate the antibacterial activity of the dental adhesives. Fig. 5A displays a schematic drawing of the steps to use human saliva as inoculum for a microcosm biofilm model. In Fig. 5B, the results of metabolic activity are presented. G_{CTRL}, $G_{2.5\%}$ and $G_{5\%}$ showed no difference among them ($p > 0.05$) and higher values compared to $G_{7.5\%}$ ($p < 0.05$). The addition of the ZnO nanoparticles at 7.5 % led to a 50 % reduction in the metabolic activity of the microorganisms in the biofilm formed on sample surfaces. Fig. 5C–E plots the CFU counting results achieved for (C) total microorganisms, (D) total streptococci, and (E) mutans streptococci, respectively. In Fig. 5D, there was no difference among groups up to 5 wt.% of ZnO addition for total microorganism viability ($p > 0.05$). The group with 7.5 wt.% of ZnO showed the lowest value of CFU/mL for total microorganisms ($p < 0.05$). For the evaluation of total streptococci (5D), there was no difference among groups ($p > 0.05$). For total mutans, streptococci counting (Fig. 5E), $G_{7.5\%}$ showed lower viability than other groups ($p < 0.05$). Microscopy images of live/dead assay (Fig. 5F–I) show that with increasing the ZnO concentration from 0 to 7.5 wt.%, more pronounced areas of dead microorganisms represented by orange/yellow color are presented within the biofilms grown over the adhesives. Note absence or minimal presence of denoted orange/yellow color in the images of control group (Fig. 5F).

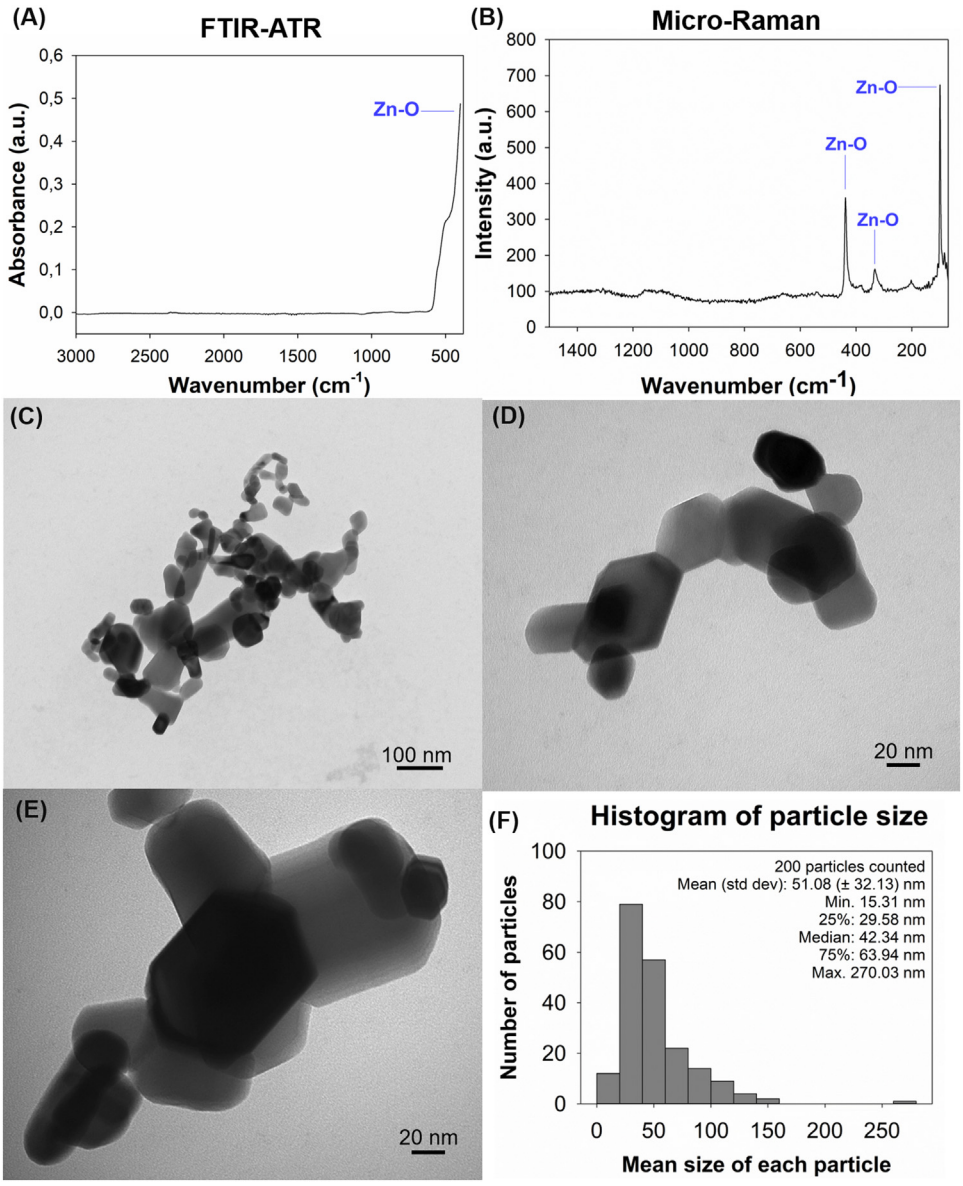

Fig. 2 – FTIR spectrum (A) and micro-Raman spectrum (B) of ZnO nanoparticles clearly indicating peaks of Zn-O bonding. The images below are from TEM analysis of ZnO nanoparticles with 30,000 (C), 110,000 (D) and 110,000 (E) magnification from different areas. The particles presented irregular shape, with non-normal size distribution (F), and they were arranged in agglomerates of nanoparticles.

4. Discussion

The addition of high concentrations of inorganic fillers changes the physicochemical properties of adhesive resins limiting their application. In this study, we observed that ZnO addition decreased the degree of conversion and flexural strength in a dose-dependent manner with its reliability for application. Further, the highest concentration of ZnO was able to inhibit the biofilm formation on the adhesive resins' surfaces.

In the radical polymerization of resin-based restorative materials, double carbon bonds (C=C) in the aliphatic chain convert to single bonds (C—C), creating polymers with improved properties compared to the uncured resin [44]. The polymerization behavior can be affected by many factors, such as the concentration of initiators, photo-exposition time [45], degree of functionality of the monomers used [35], resins' viscosity [35], and transmission of light through the material [46]. A high monomer to polymer conversion is desired to provide high mechanical strength [35] and hardness [47], besides reliable hydrolytic stability for resin-based restorative materials [35,48]. The increasing of ZnO concentration clearly led to decreased DC (Fig. 3C and D). It is a limitation of this study not to evaluate the polymerization kinetics of the adhesives. However, it is possible to venture to state that a high mass fraction of ZnO leads to a high viscosity in the resin blend, which may be decreasing the monomers' chain mobility, delaying the

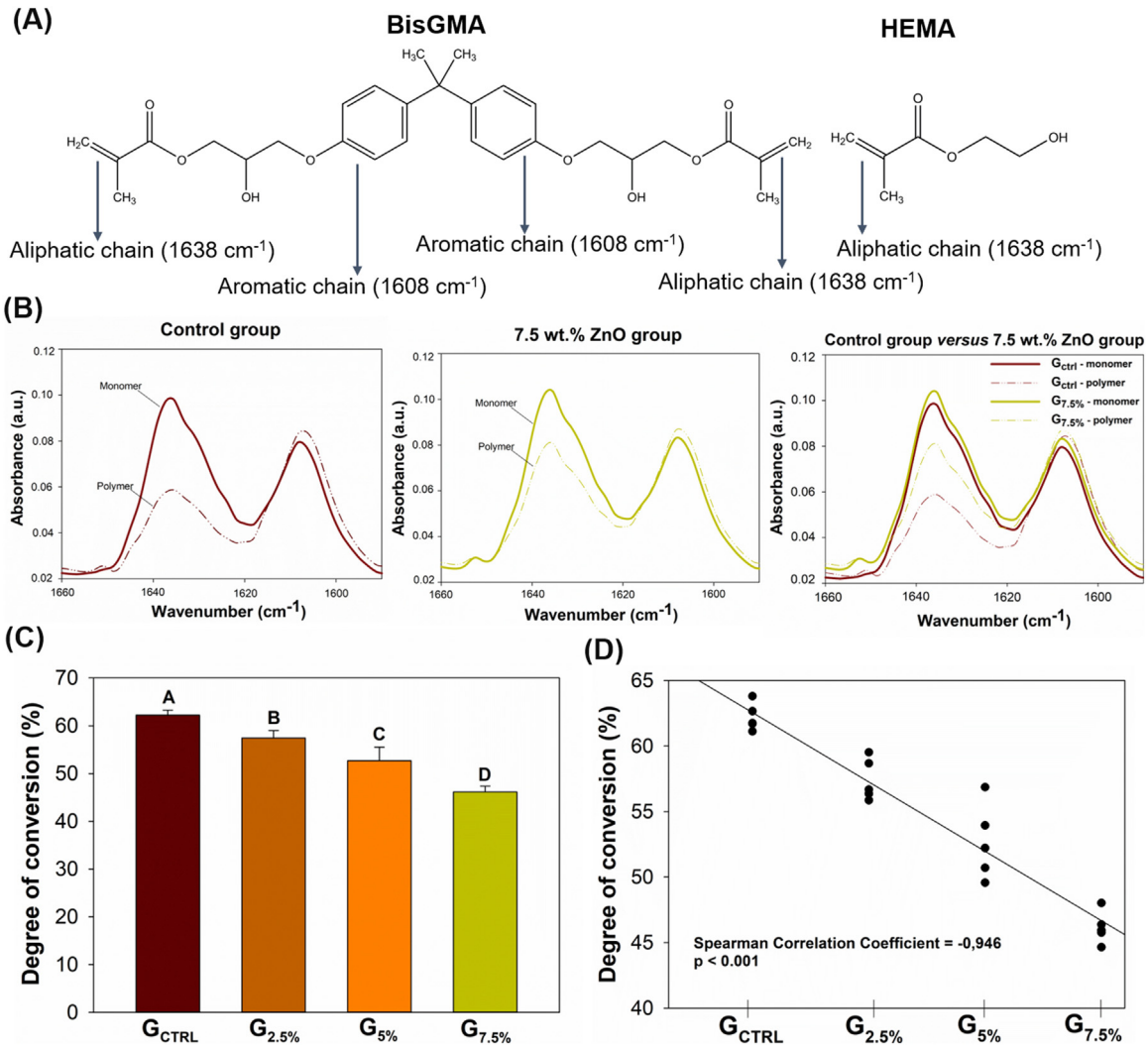

Fig. 3 – Chemical structure of the two monomers used to formate the experimental dental adhesives: bisphenol A glycerolate dimethacrylate (BisGMA) and 2-hydroxyethyl methacrylate (HEMA) (A). The arrows indicate in which wavelength (nm) it is possible to identify the cabon-carbon double bonds of the monomers in the aliphatic (1638 cm^{-1}) or aromatic chain (1608 cm^{-1}). The graphs in (B) show the FTIR spectra of DC from monomer to polymer from one sample of G_{CTRL} and one sample of $G_{7.5\%}$ to illustrate the variation of peaks high, which was used to calculate the DC. It is possible to observe the higher difference in the aliphatic peak (1638 cm^{-1}) from monomer to polymer for G_{CTRL} in comparison to the difference of high observed for $G_{7.5\%}$ (Control group versus 7.5 wt.% ZnO group image). There was statistically significant difference among groups ($p < 0.05$), indicated by different uppercase letters in the graph (C), and strong negative correlation between filler content and DC (D), evidencing that by increasing the ZnO concentration, the DC was lower.

polymerization kinetics [35,49], lowering the maximum polymerization rate [4], and reducing the DC. Other detrimental factor associated to the decrease in DC is the limited light penetration due to the higher opacity of filled resins [46]. Despite the lower values, all groups achieved mean DC above 50%, which is similar to the results found for commercial adhesives [50].

The mechanical behavior of the tested formulations was also evaluated by flexural strength and elastic modulus. Prior to the decision about the concentrations of ZnO tested in this study; we also analyzed the resin's flexural strength with 10 wt.% of ZnO. At this concentration, the adhesive's samples presented high resilience, not allowing to obtain values of resistance at the moment of fracture. Even though physical properties can be positively related to the DC [35,46], $G_{7.5\%}$ was the only group that showed statistical difference for the mechanical properties in comparison to the G_{CTRL}. It is well known that the decrease of particles' size to nanoscale leads to their agglomeration due to the higher surface/volume ratio. In the present research, the nanopowder was arranged in agglomerates as observed via TEM analysis. It is not easy to keep these particles non-agglomerated by manually or mechanical mixing without stabilizers [4] or electrostatic repulsion [33]. Therefore, $G_{7.5\%}$ may have presented more agglomerates able to act as stress concentration defect sites,

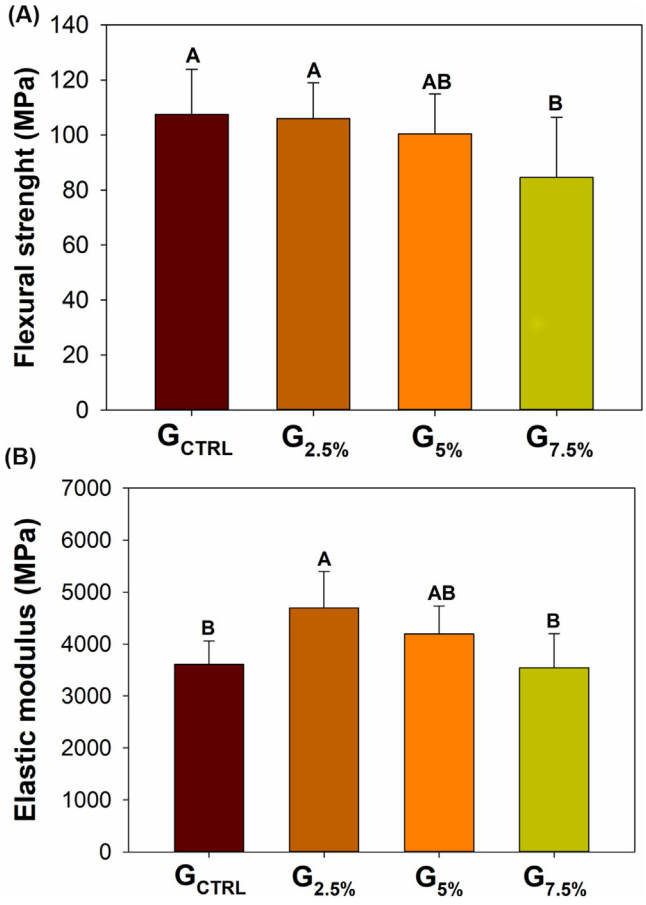

Fig. 4 – Graphs of flexural strength (MPa) (A) and elastic modulus (MPa) (B) of the experimental dental adhesives with different concentrations of ZnO nanoparticles. Different uppercase letters indicate statistically significant difference among groups ($p < 0.05$), showing that $G_{7.5\%}$ had lower values in both tests in comparison to G_{CTRL}.

impairing the stress dissipation, and turning the polymer more prone to mechanical failure [51].

Interestingly, the elastic modulus of the adhesives increased for $G_{2.5\%}$ in comparison to G_{CTRL}. Despite there was no statistical difference for flexural strength for $G_{2.5\%}$, the particles in this group may have reinforced the polymer via crack deflection and plastic deformation in the area surrounded the fillers [51] or increased the rigidity of the blend because of the higher inorganic/organic proportion in $G_{2.5\%}$ in comparison to G_{CTRL}. On the one hand, the addition of the highest ZnO concentration affected both mechanical properties; instead, incoorporating up to 5 wt.% showed no differences compared to G_{CTRL}. Even so, $G_{7.5\%}$ still presented suitable DC and flexural strength in accordance with ISO 4049 (50 MPa for polymer-based restorative materials, type 2, class 2, group 1) [36].

Recurrent caries is influenced by the presence of proper marginal sealing, bonding interface stability, the magnitude of bacterial penetration, application of mechanical forces on the restored structure, and patient-related variables [52]. This event leads to further loss of tooth tissues, which can damage the remaining structure and may lead to the tooth's premature loss. Unlike what was believed years ago, residual bacteria in dentin does not represent a concern anymore, since they are killed over time due to the lack of available nutrients when there is an effective marginal sealing [53]. The purpose of adding antibacterial agents in restorative materials is to protect the structure against biofilm formation at the interface and to act against material degradation and dental demineralization from biofilm products [54]. In vivo, previous the attachment of bacteria to the solid structures, proteins are adsorbed and occur to form a coating on the surfaces [55]. This feature is an important factor to be reproduced in vitro. For this reason, it was recently mentioned the necessity of standardized approaches to evaluate the interactions between biomaterials and biofilms [31]. Besides the concern about the biofilm model used, other conditions related to these interactions are not reproduced in vitro, such as the formation of acquired pellicle from saliva on the restorative materials [30]. When placed in the oral environment, solid surfaces (such as those from teeth and restorative materials) are covered by this film, which is developed via adsorption of salivary macromolecules [30] and influences the adhesion of microorganisms on the surfaces [56]. To the best of our knowledge, there is no evaluation of resin-based restorative materials with ZnO after the formation of the acquired pellicle.

Besides the acquired pellicle saliva, another important issue regarding the assays used to test antibacterial dental materials is the complexity of the chosen biofilm model.

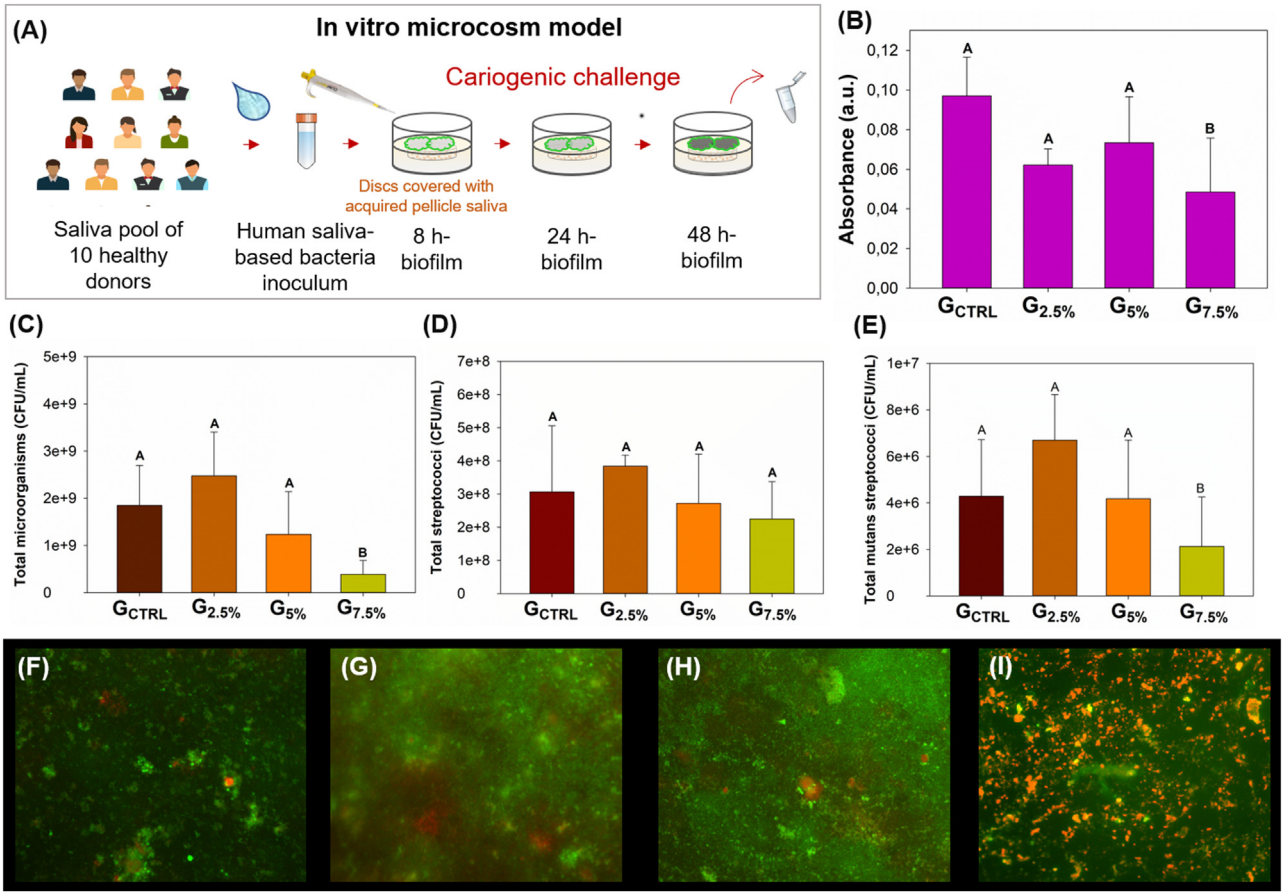

Fig. 5 – Image (A) illustrates the methods applied in the present study to form the biofilms on samples' surfaces. Saliva from ten healthy donors was used to obtain the inoculum. Moreover, the samples were covered by saliva to form the acquired pellicle, followed by the contact with the bacteria and maturation for 48 h. The graph in (B) shows the statistically significant difference among groups for metabolic activity of the total microorganisms in the biofilms via MTT analysis. The graphs in (C), (D) and (E) present the results of CFU/mL found for total microorganisms, total streptococci and total mutans streptococci, respectively. The different uppercase letters in each graph indicate statistically significant difference among groups for each microorganism evaluated ($p < 0.05$). The images from (F) to (I) present the results of live/dead staining and analysis via microscopy. From (F) to (I) the ZnO concentration increases (G_{CTRL} to $G_{7.5\%}$) and more areas associated to microorganisms with damaged membranes are evidenced with higher amounts of ZnO.

In many antibacterial assays, the inoculum is usually composed of an single-species of *Streptococcus mutans* [31] due to the positive correlation between these bacteria and caries development [57]. Nevertheless, *Streptococcus mutans* biofilms display properties that are dramatically distinct from their planktonic counterparts, including much higher resistance to antibacterial approaches, making the biofilm much more challenging to kill than planktonic bacteria [58]. Unfortunately, we poorly know how antibacterial restorative materials behave in an oral environment since there is a massive lack of in situ and in vivo studies about this subject. Therefore, we aimed to evaluate the antibacterial effect of intended formulations using a more robust and complex model. Unlike previous studies that evaluated dental materials with ZnO, we observed statistical differences in the colonies counting (Fig. 5C and E) and metabolic activity (Fig. 5B) only when 7.5 wt.% of ZnO was added in comparison to G_{CTRL}. The acquired pellicle saliva formed on samples' surfaces, the use of saliva-derived multi-species biofilm, and the maturation for 48 h are probably the key factors that led to the differences found here in comparison to previous studies, when lower concentrations of ZnO, such as 1–6 wt.% [14,18,20,21,25,26,59], induced antibacterial activity.

In the counting of viable colonies, three different media were used to select the microorganisms in total microorganisms, total streptococci, and mutans streptococci. Interestingly, we did not observe a statistical difference for total streptococci in MSA, but there was a statistical difference when *Streptococcus mutans* were isolated in MSB. Moreover, when analyzing all microorganisms in the TSA, there was also a statistical difference for $G_{7.5\%}$ compared to other groups. The antibacterial activity of ZnO is well established. This effect occurs through damage to the molecular structure of bacterial membrane phospholipids, subsequent internalization of the particles into the cytoplasmatic matrix [60], and development of reactive oxygen species (superoxide radical ($O_2^{-}\bullet$),

hydroxyl radicals (OH•) and singlet oxygen ($^1O_2$)) on ZnO surfaces [9]. Moreover, in water, ZnO may release Zn^{+2}, which can also be responsible for its antibacterial activity [61]. We suggest that further studies evaluate these particles' antibacterial activity using the high-challenge cariogenic media to investigate how long this action can be observed. The antibacterial activity of ZnO is greater, the smaller its particle size due to the higher total surface area available to interact with the microorganisms [19]. Hence, the results found for this study should not be considered for all ZnO nanoparticles incorporated into restorative materials, and the outcomes observed here may be different when other nanoparticles are applied. Even so, we chose to evaluate a commercial particle of ZnO because it is easier to be commercially acquired and most likely to be used.

Finally, other studies assessed the antimicrobial activity of restorative materials with ZnO by only one method [15,19,21,23], which may offer us low-quality evidence regarding the antibacterial effects agent. In this study, we also evaluated the materials concerning the metabolic activity of the biofilms developed on adhesives' surfaces, and qualitatively investigated them via microscopy using the BacLight LIVE/DEAD dyes. Biofilms can show low metabolic but are still viable [62]. Furthermore, the antibacterial agents can modify viability factors instead of directly killing the cells, decreasing the metabolic activity, but not directly reducing the cell viability [62]. The metabolic activity assays should always be performed in association with other tests such as cell counting to address the issue of weakly understanding of the antibacterial mechanism.

Future studies are warranted to address the incorporation of ZnO nanoparticles and their antibacterial and bioactivity behavior. Especially when new levels of complexity and challenges are provided to help predict novel antimicrobial materials' performance in vivo and evaluate their long-term bonding properties.

5. Conclusion

In summary, our findings demonstrate that ZnO nanoparticles at 7.5% promote a substantial bacterial reduction of biofilms. This was achieved against a 48h mature saliva-derived oral microcosm biofilm. The addition of 7.5 wt.% of ZnO affected the chemical and mechanical properties of the dental adhesive. However, the DC was comparable to the reported DC values of commercial adhesives, and the flexural strength was within the ISO recommended range. ZnO can be a potential multiapproach for bioactivity for the next generation of dental adhesives.

Funding

This research did not receive any specific grant from funding agencies in the public, commercial, or not-for-profit sectors.

Conflict of interest

None declared.

Acknowledgments

The authors are grateful to the volunteers for their participation in this study. We are grateful to Esstech (Essington, PA) for kindly donating the BisGMA and TEGDMA monomers. AAB and MSI acknowledge the scholarship during their Ph.D. studies from the Imam AbdulRahman bin Faisal University, Dammam, Saudi Arabia, and the Saudi Arabia Cultural Mission. IMG acknowledge the scholarship during their Ph.D. studies from the Coordenação de Aperfeiçoamento de Pessoal de Nível Superior - Brasil (CAPES) - Finance Code 001 – scholarship. We also thank the University of Maryland School of Medicine Center for Innovative Biomedical Resources-Baltimore, Maryland-UMB Electron Microscopy Core Imaging Facility on behalf Dr. Ru-ching Hsia for assistance with TEM.

REFERENCES

[3] Genari B, Leitune VCB, Jornada DS, Camassola M, Arthur RA, Pohlmann AR, et al. Antimicrobial effect and physicochemical properties of an adhesive system containing nanocapsules. Dent Mater 2017;33:735–42.
[4] Garcia IM, Souza VS, Hellriegel C, Scholten JD, Collares FM. Ionic liquid-stabilized titania quantum dots applied in adhesive resin. J Dent Res 2019;98:682–8.
[5] Moszner N, Salz U, Zimmermann J. Chemical aspects of self-etching enamel-dentin adhesives: a systematic review. Dent Mater 2005;21:895–910.
[6] Osorio R, Osorio E, Medina-Castillo AL, Toledano M. Polymer nanocarriers for dentin adhesion. J Dent Res 2014;93:1258–63.
[7] Qayyum S, Khan AU. Nanoparticles vs. biofilms: a battle against another paradigm of antibiotic resistance. MedChemComm 2016;7:1479–98.
[8] Niu LN, Zhang W, Pashley DH, Breschi L, Mao J, Chen JH, et al. Biomimetic remineralization of dentin. Dent Mater 2014;30:77–96.
[9] Mirzaei HDM. Zinc oxide nanoparticles: biological synthesis and biomedical applications. Ceram Int 2017;43:907–14.
[10] Ordinola-Zapata R, Bramante CM, Garcia-Godoy F, Moldauer BI, Gagliardi Minotti P, Tercilia Grizzo L, et al. The effect of radiopacifiers agents on pH, calcium release, radiopacity, and antimicrobial properties of different calcium hydroxide dressings. Microsc Res Technol 2015;78:620–5.
[11] Osorio R, Cabello I, Toledano M. Bioactivity of zinc-doped dental adhesives. J Dentist 2014;42:403–12.
[12] Toledano M, Perez-Alvarez MC, Aguilera FS, Osorio E, Cabello I, Toledano-Osorio M, et al. A zinc oxide-modified hydroxyapatite-based cement facilitated new crystalline-stoichiometric and amorphous apatite precipitation on dentine. Int Endod J 2017;50(Suppl. 2):e109–19.
[13] Mutoh N, Tani-Ishii N. A biocompatible model for evaluation of the responses of rat periapical tissue to a new zinc oxide-eugenol sealer. Dent Mater J 2011;30:176–82.
[14] Garcia IM, Leitune VCB, Visioli F, Samuel SMW, Collares FM. Influence of zinc oxide quantum dots in the antibacterial activity and cytotoxicity of an experimental adhesive resin. J Dentist 2018;73:57–60.
[15] Wang J, Du L, Fu Y, Jiang P, Wang X. ZnO nanoparticles inhibit the activity of *Porphyromonas gingivalis* and *Actinomyces naeslundii* and promote the mineralization of the cementum. BMC Oral Health 2019;19:84.

[16] Angel Villegas N, Silvero Compagnucci MJ, Sainz Aja M, Rocca DM, Becerra MC, Fabian Molina G, et al. Novel antibacterial resin-based filling material containing nanoparticles for the potential one-step treatment of caries. J Healthc Eng 2019;2019:6367919.
[17] Nguyen TMT, Wang PW, Hsu HM, Cheng FY, Shieh DB, Wong TY, et al. Dental cement's biological and mechanical properties improved by ZnO nanospheres. Mater Sci Eng C Mater Biol Appl 2019;97:116–23.
[18] Mahshid Saffarpour MR, Tahriri M, Peymani A. Antimicrobial and bond strength properties of a dental adhesive containing zinc oxide nanoparticles. Braz J Oral Sci 2016;15:66–9.
[19] Raghupathi KR, Koodali RT, Manna AC. Size-dependent bacterial growth inhibition and mechanism of antibacterial activity of zinc oxide nanoparticles. Langmuir 2011;27:4020–8.
[20] Tavassoli Hojati S, Alaghemand H, Hamze F, Ahmadian Babaki F, Rajab-Nia R, Rezvani MB, et al. Antibacterial, physical and mechanical properties of flowable resin composites containing zinc oxide nanoparticles. Dent Mater 2013;29:495–505.
[21] Niu LN, Fang M, Jiao K, Tang LH, Xiao YH, Shen LJ, et al. Tetrapod-like zinc oxide whisker enhancement of resin composite. J Dent Res 2010;89:746–50.
[22] Eshed M, Lellouche J, Matalon S, Gedanken A, Banin E. Sonochemical coatings of ZnO and CuO nanoparticles inhibit *Streptococcus mutans* biofilm formation on teeth model. Langmuir 2012;28:12288–95.
[23] Brayner R, Ferrari-Iliou R, Brivois N, Djediat S, Benedetti MF, Fievet F. Toxicological impact studies based on Escherichia coli bacteria in ultrafine ZnO nanoparticles colloidal medium. Nano Lett 2006;6:866–70.
[24] Spencer CG, Campbell PM, Buschang PH, Cai J, Honeyman AL. Antimicrobial effects of zinc oxide in an orthodontic bonding agent. Angle Orthod 2009;79:317–22.
[25] Kasraei S, Sami L, Hendi S, Alikhani MY, Rezaei-Soufi L, Khamverdi Z. Antibacterial properties of composite resins incorporating silver and zinc oxide nanoparticles on *Streptococcus mutans* and Lactobacillus. Restor Dent Endod 2014;39:109–14.
[26] Wang Y, Hua H, Li W, Wang R, Jiang X, Zhu M. Strong antibacterial dental resin composites containing cellulose nanocrystal/zinc oxide nanohybrids. J Dentist 2019;80:23–9.
[27] Leitune VCB, Schiroky PR, Genari B, Camassola MS, Samuel SMW, et al. Nanoneedle-like zinc oxide as a filler particle for an experimental adhesive resin. Indian J Dent Res 2019;30:777–82.
[28] Marsh PD, Zaura E. Dental biofilm: ecological interactions in health and disease. J Clin Periodontol 2017;44(Suppl. 18):S12–22.
[29] Hoiby N, Bjarnsholt T, Givskov M, Molin S, Ciofu O. Antibiotic resistance of bacterial biofilms. Int J Antimicrob Agents 2010;35:322–32.
[30] Gong K, Mailloux L, Herzberg MC. Salivary film expresses a complex, macromolecular binding site for *Streptococcus sanguis*. J Biol Chem 2000;275:8970–4.
[31] Kreth J, Ferracane JL, Pfeifer CS, Khajotia S, Merritt J. At the interface of materials and microbiology: a call for the development of standardized approaches to assay biomaterial-biofilm interactions. J Dent Res 2019;98:850–2.
[33] Garcia IM, Leitune VC, Kist TL, Takimi A, Samuel SM, Collares FM. Quantum dots as nonagglomerated nanofillers for adhesive resins. J Dent Res 2016;95:1401–7.
[34] Rodrigues SB, Gamba PC, Leitune D, Collares VCBFM. Acrylamides and methacrylamides as alternative monomers for dental adhesives. Dent Mater 2018;34:1634–44.
[35] Collares FM, Ogliari FA, Zanchi CH, Petzhold CL, Piva E, Samuel SM. Influence of 2-hydroxyethyl methacrylate concentration on polymer network of adhesive resin. J Adhes Dent 2011;13:125–9.
[36] Standardization IOf. ISO 4049. Dentistry: polymer-based restorative materials; 2009. p. 1–28.
[37] de Melo MA, Passos VF, Lima JP, Parente GC, Rodrigues LK, Santiago SL. Erosive potential of processed and fresh orange juice on human enamel. J Dentist Children 2015;82:10–5.
[38] Melo MA, Wu J, Weir MD, Xu HH. Novel antibacterial orthodontic cement containing quaternary ammonium monomer dimethylaminododecyl methacrylate. J Dentist 2014;42:1193–201.
[39] McBain AJ. In vitro biofilm models: an overview. Adv Appl Microbiol 2009;69:99–132 [chapter 4].
[40] Raevskaya AEYVP, Stroyuk OLS, Kuchmiy Ya, Dzhagan VM, Milekhin AG, Yeryukov NA, et al. Spectral and luminescent properties of ZnO–SiO2 core–shell nanoparticles with size-selected ZnO cores. RSC Adv 2014;4:63393–401.
[41] Rasha N, Moussawi DP. Modification of nanostructured ZnO surfaces with curcumin: fluorescence-based sensing for arsenic and improving arsenic removal by ZnO. RSC Adv 2016;6:17256–68.
[42] Mihaila M. Correlations phonon spectrum-sensitivity in metal-oxide gas sensors. Proc Eng 2014;87:1609–12.
[43] Víctor Herrera TD-B, Eric R-C, Godofredo G-S, Reina G, Crisóforo M, Enrique R, et al. Highly visible photoluminescence from Ta-doped structures of ZnO films grown by HFCVD. Crystals 2018;8:1–18.
[44] Andrzejewska E. Photopolymerization kinetics of multifunctional monomers. Prog Polym Sci 2001;26:605–65.
[45] Stansbury JW, Dickens SH. Determination of double bond conversion in dental resins by near infrared spectroscopy. Dent Mater 2001;17:71–9.
[46] Shortall AC. How light source and product shade influence cure depth for a contemporary composite. J Oral Rehabil 2005;32:906–11.
[47] Ferracane JL. Correlation between hardness and degree of conversion during the setting reaction of unfilled dental restorative resins. Dent Mater 1985;1:11–4.
[48] Ferracane JL. Hygroscopic and hydrolytic effects in dental polymer networks. Dent Mater 2006;22:211–22.
[49] Barszczewska-Rybarek IM. Characterization of urethane-dimethacrylate derivatives as alternative monomers for the restorative composite matrix. Dent Mater 2014;30:1336–44.
[50] Gaglianone LA, Lima AF, Goncalves LS, Cavalcanti AN, Aguiar FH, Marchi GM. Mechanical properties and degree of conversion of etch-and-rinse and self-etch adhesive systems cured by a quartz tungsten halogen lamp and a light-emitting diode. J Mech Behav Biomed Mater 2012;12:139–43.
[51] Renan Belli SK, Petschelt A, Hornberger H, Boccaccini AR, Ulrich L. Strengthening of dental adhesives by particle reinforcement. J. Mech. Behav. Biomed. Mater 2014;37:100–8.
[52] Ferracane JL. Models of caries formation around dental composite restorations. J Dent Res 2017;96:364–71.
[53] Corralo DJ, Maltz M. Clinical and ultrastructural effects of different liners/restorative materials on deep carious dentin: a randomized clinical trial. Caries Res 2013;47:243–50.
[54] Kusuma Yulianto HD, Rinastiti M, Cune MS, de Haan-Visser W, Atema-Smit J, Busscher HJ, et al. Biofilm composition and composite degradation during intra-oral wear. Dent Mater 2019;35:740–50.
[55] Busscher HJ, Rinastiti M, Siswomihardjo W, van der Mei HC. Biofilm formation on dental restorative and implant materials. J Dent Res 2010;89:657–65.

[56] Imazato S, Ebi N, Takahashi Y, Kaneko T, Ebisu S, Russell RR. Antibacterial activity of bactericide-immobilized filler for resin-based restoratives. Biomaterials 2003;24: 3605–9.
[57] Kirstila V, Hakkinen P, Jentsch H, Vilja P, Tenovuo J. Longitudinal analysis of the association of human salivary antimicrobial agents with caries increment and cariogenic micro-organisms: a two-year cohort study. J Dent Res 1998;77:73–80.
[58] Melo MAS, Weir MD, Passos VF, Rolim JPM, Lynch CD, Rodrigues LKA, et al. Human in situ study of the effect of bis(2-methacryloyloxyethyl) dimethylammonium bromide immobilized in dental composite on controlling mature cariogenic biofilm. Int J Mol Sci 2018:19.
[59] Aydin Sevinc B, Hanley L. Antibacterial activity of dental composites containing zinc oxide nanoparticles. J Biomed Mater Res B Appl Biomater 2010;94:22–31.
[60] Huang Z, Zheng X, Yan D, Yin G, Liao X, Kang Y, et al. Toxicological effect of ZnO nanoparticles based on bacteria. Langmuir 2008;24:4140–4.
[61] Leung YH, Xu X, Ma AP, Liu F, Ng AM, Shen Z, et al. Toxicity of ZnO and TiO2 to *Escherichia coli* cells. Sci Rep 2016;6:35243.
[62] Lin NJ. Biofilm over teeth and restorations: what do we need to know? Dent Mater 2017;33:667–80.
[63] Melo Mary Anne. Share nanotechnology-based restorative materials for dental caries management. Trends Biotechnol 2013, http://dx.doi.org/10.1016/j.tibtech.2013.05.010.